

# Development of Heated Narrow Channels with Enhanced Liquid Supply in Forced Convective Boiling

Yukihiro INADA<sup>1</sup>, Shinichi MIURA<sup>1</sup>, Kenta HARA<sup>1</sup>, Yasuhisa SHINMOTO<sup>1</sup> and Haruhiko OHTA<sup>1</sup>

<sup>1</sup> Dept. Aeronautics and Astronautics, Kyushu University, Fukuoka, Japan, ohta@aero.kyushu-u.ac.jp

## Abstract

Heat generation density from semiconductor devices increases with the rapid development of electronic technology. The cooling system using boiling two-phase phenomena attracts much attention because of its high heat removal potential. Most of heat transfer researches concerning the development of electronic devices are conducted for the cooling of small semiconductor chips, while there are limited numbers of innovative investigations for the cooling of a large area at extremely high heat flux larger than  $2 \times 10^6 \text{ W/m}^2$ . The technology can be applied to the cooling systems in space, e.g., cooling of laser medium in solar power satellites when solar energy is converted to laser power. To develop compact and high-performance cooling systems, a structure of narrow heated channel between parallel plates with auxiliary unheated channel was devised and tested by using water in three different kinds of experimental conditions. One of liquid supply method, where liquid is supplied to both of the main heated and the auxiliary unheated channel keeping the exit of the auxiliary channel closed, gives the highest CHF value at total volumetric flow rates more than  $3.0 \times 10^{-5} \text{ m}^3/\text{s}$  and 2mm gap size of main heated channel.

## 1. Introduction

Recent development in electronic devices with increased heat dissipation requires severe cooling conditions and an efficient method for heat removal is needed for the cooling under high heat flux conditions. Most of existing researches in this discipline are performed for the cooling of small semi-conductors, while almost no innovative research is directed for the cooling of power electronics where large amount of heat is dissipated at high heat flux from a large area.

As there is limitation in the performance of air cooling method, it is needed to develop liquid cooling technologies. In addition, a two-phase fluid system, which has high heat removal ability due to the latent heat transportation, is a promising method for high performance cooling systems.

The objective of this study is to develop methods for the removal of dissipated heat at extremely high heat flux larger than  $1 \times 10^6 \text{ W/m}^2$  ( $100 \text{ W/cm}^2$ ) from a large area with a heated length larger than 150mm. To increase critical heat flux (CHF) for flow boiling in rectangular narrow channels, a method of liquid supply is devised to prevent dryout which usually occurs in the downstream region.

Many works on critical heat flux have been undertaken in rectangular channels. Monde et al. performed boiling experiments for vertical upward flow using water at atmospheric pressure<sup>1)</sup>. CHF values decreased with increasing of  $L/s$ , where  $L$  is a length and  $s$  is a gap size of a heated channel. Bonjour and Lallemand experimented using rectangular channels, varying gap sizes; 0.5, 1.0, 2.0mm<sup>2)</sup>. In those experiments, boiling heat transfer coefficient was improved as decreasing the gap size. Zhang, Mudawar et al. investigated flow boiling of FC-72 with changing

channels' orientation. They found that the flow direction influenced CHF values in low velocity region<sup>3)</sup>. Kim et al. also performed flow boiling experiments, varying a channel orientation and its gap size. According to the result, there exists a critical gap size enhancing the heat transfer rate at a certain surface inclination angle<sup>4)</sup>.

The cooling system developed here can be applied to the space solar power system (SSPS) where a large amount of heat is generated from laser medium with a large size, for example, of  $1 \text{ m}^2$ . The energy conservation and global environmental protection are simultaneously promoted by the application of the present research<sup>5)</sup> for the cooling of power conversion systems using SiC semiconductors in the next generation on ground.

## 2. Experimental Apparatus

There are some possible methods to increase CHF values in rectangular narrow heated channels, e.g. high-subcooled boiling or microbubble emission boiling (MEB) by changing inlet liquid conditions<sup>6)</sup>, and using self-wetting behaviors by mixtures where surface tension gradient due to concentration (and temperature) gradient(s) promotes the supply of liquid underneath bubbles<sup>7)</sup>.

In the present study, we focus on the structure of heated narrow channels to develop cold plates of high-performance cooling system. The schematic view of devised structure is given in **Fig.1**. The test section assembly has two narrow rectangular channels, i.e. a main heated channel and an auxiliary unheated channel located behind the main heated channel. The structure is devised to prevent burnout by the aid of enhanced liquid supply from the auxiliary unheated channel.

The test section is shown in **Fig.2**. Liquid is supplied additionally via sintered metal porous plates located at

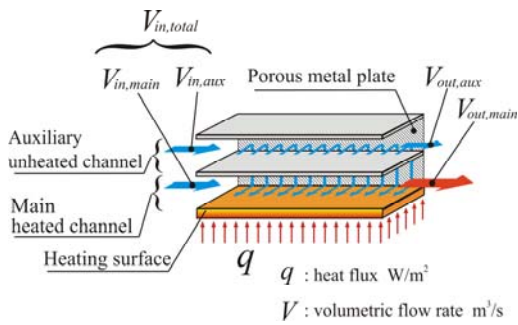


**Fig.1** Schematic view of devised structure.

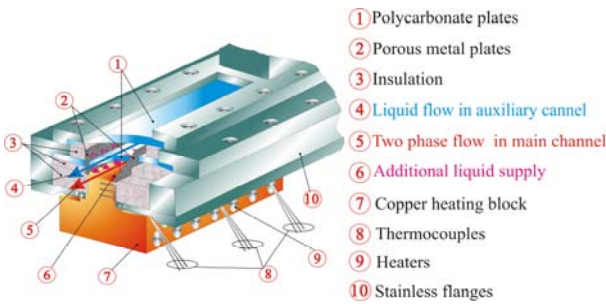


**Fig.2** Test section.

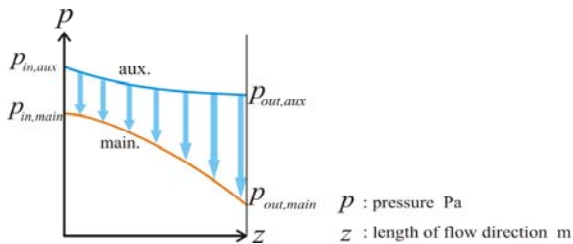


**Fig.3** Expected pressure distributions in both channels.

both sides of the main heated channel. This additional liquid supply is realized by local pressure differences between auxiliary unheated channel and main heated channel as shown qualitatively in **Fig.3**. The structure reduces heated length substantially to half width of the present segment channel because the liquid is supplied directly in the transverse direction perpendicular to the flow in the main heated channel. The segment channels with a small width are assembled to construct parallel channels to realize a large cooling area also in the transverse direction to the flow in the main heated channels. A heating surface of 150mmL ×30mmW has arrays of grooves with apex angle of 90 deg and a pitch of 1mm to supply liquid to the center of the heating surface from the side of the main heated channel by the capillary pressure difference. The generated flattened bubbles in the gap of main heated channel squeeze the liquid-vapor interface to realize high heat transfer coefficient due to the evaporation of thin films formed in the grooves.

Heat flux is supplied from the cartridge heaters

inserted in the bottom of a copper heating block. In the block, thermocouples are inserted at three different locations along a center line, i.e.,  $z=25\text{mm}$  (upstream center, U-C),  $z=75\text{mm}$  (midstream center, M-C),  $z=125\text{mm}$  (downstream center, D-C) from the upstream (bottom) edge of the heating surface, and at a side location  $z=75\text{mm}$  (midstream side, M-S) with a distance of 9mm from the center line. The depths of thermocouples are 3mm, 10mm and 17mm from the apices of grooves. The surface heat flux and surface temperature are defined at a hypothetical plane contacting the apices of grooves. Heat flux is evaluated based on the nominal surface area ignoring the existence of grooves.

Fluid temperatures are measured at the inlet and the outlet of the main heated channel by thermocouples. Pressure data are obtained by pressure transducers at the inlet and the outlet in both channels (total 4 points). Test loop is shown in **Fig.4**.

### 3. Experimental Conditions

The objective of this paper is to increase CHF values by the improvement of liquid supply to the heating surface. Three different experiments are performed. All experiments are performed for vertical upward flow on ground.

**Experiment A** is performed under conditions that the inlet of main heated channel and the outlet of auxiliary unheated channel were closed as shown in **Fig.5** to clarify effects of additional liquid supply from auxiliary unheated channel. Experimental conditions are listed in **Table 1**.

**Experiment B** is performed without additional liquid supply from auxiliary unheated channel, i.e. fluid flows is limited in the main heated channel as shown in **Fig.6**. Experimental conditions are shown in **Table 2**.

**Experiment C** is performed under conditions that only outlet of auxiliary unheated channel is closed as shown in **Fig.7**. The inlet volumetric flow rates for both channels are the same at heat flux  $3.0 \times 10^5 \text{ W/m}^2$ , and the distribution of flow rates is not adjusted at higher heat fluxes tested. Experimental conditions are shown in **Table 3**.

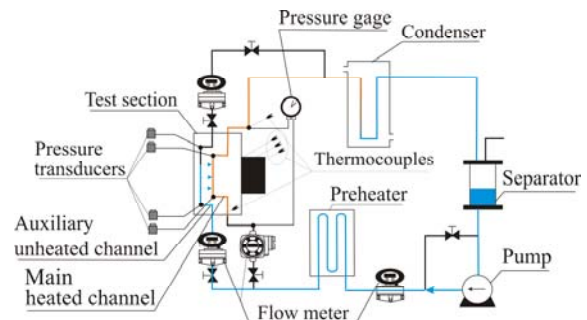


**Fig.4** Test loop.

**Table 1** Conditions for Experiment A.

Test liquid	Water
Gap size of main heated channel	$s_{main}=2$ mm, 5 mm
Gap size of auxiliary unheated channel	$s_{aux}=10$ mm
Inlet volumetric flow rate of main channel	$V_{in,main}=0$ m <sup>3</sup> /s
Outlet volumetric flow rate of auxiliary channel	$V_{out,aux}=0$ m <sup>3</sup> /s
Total inlet volumetric flow rate	$V_{in,total}=1.5 \times 10^{-5}$ - $6.0 \times 10^{-5}$ m <sup>3</sup> /s
Inlet liquid subcooling	$\Delta T_{sub,in}=15$ K
Pressure range in test section	$P=0.13$ - $0.16$ MPa

**Table 2** Conditions for Experiment B.

Test liquid	Water
Gap size of main heated channel	$s_{main}=2$ mm, 5 mm
Total inlet volumetric flow rate	$V_{in,total}=1.5 \times 10^{-5}$ - $6.0 \times 10^{-5}$ m <sup>3</sup> /s
Inlet liquid subcooling	$\Delta T_{sub,in}=15$ K
Pressure range in test section	$P=0.11$ - $0.19$ MPa

**Table 3** Conditions for Experiment C.

Test liquid	Water
Gap size of main heated channel	$s_{main}=2$ mm, 5 mm
Gap size of auxiliary unheated channel	$s_{aux}=10$ mm
Outlet volumetric flow rate of auxiliary channel	$V_{out,aux}=0$ m <sup>3</sup> /s
Total inlet volumetric flow rate	$V_{in,total}=1.5 \times 10^{-5}$ - $4.5 \times 10^{-5}$ m <sup>3</sup> /s
Inlet liquid subcooling	$\Delta T_{sub,in}=15$ K
Pressure range in test section	$P=0.11$ - $0.18$ MPa

## 4. Experimental Results and Discussion

### 4.1 Critical Heat Flux

**Fig. 8** shows relationship between CHF values and total inlet volumetric flow rate in Experiment A to C. (i) CHF values larger than  $2.0 \times 10^6$  W/m<sup>2</sup> are obtained at  $V_{in,total}=4.5 \times 10^{-5}$  m<sup>3</sup>/s for 2mm gap size in Experiment C and  $V_{in,total}=6.0 \times 10^{-5}$  m<sup>3</sup>/s in Experiment A and B. (ii) In Experiment A, CHF values for 2mm gap size are lower than those for 5mm gap size at low total volumetric flow rates ( $V_{in,total} = 1.5, 3.0 \times 10^{-5}$  m<sup>3</sup>/s), while higher CHF values are obtained for 2mm gap size at high total volumetric flow rates ( $V_{in,total} = 4.5, 6.0 \times 10^{-5}$  m<sup>3</sup>/s). (iii) In Experiment B, no large difference in CHF values appears between 2mm and 5mm gap sizes. (iv) In Experiment C, CHF values for 2mm gap size are higher than those for 5mm gap size at the same total volumetric flow rate conditions. (v) CHF values for 2mm gap size in Experiment C are higher than those in Experiments A and B at the conditions of  $V_{in,total} = 3.0, 4.5 \times 10^{-5}$  m<sup>3</sup>/s. Therefore, the method of Experiment C is superior to those of Experiments A and B from a viewpoint of increasing CHF values.

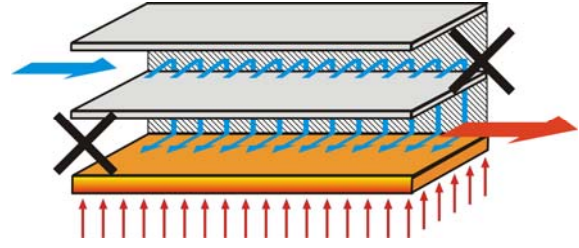


**Fig.5** Liquid supply in Experiment A.

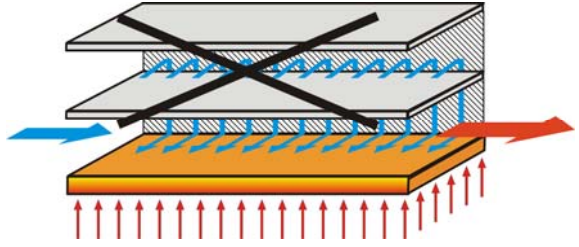


**Fig.6** Liquid supply in Experiment B.

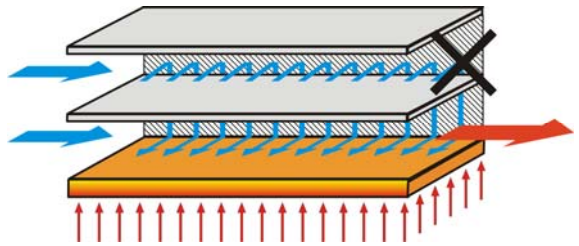


**Fig.7** Liquid supply in Experiment C.

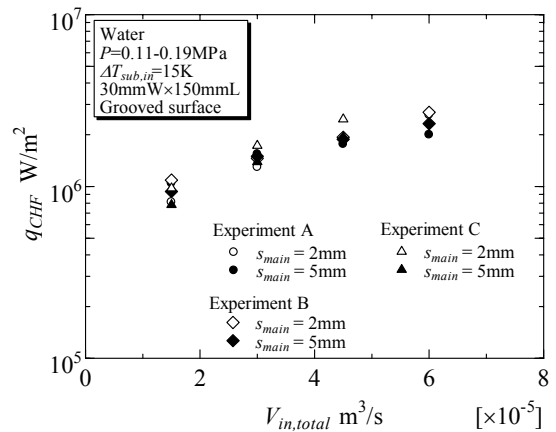


**Fig.8** CHF versus total inlet volumetric flow rate.

### 4.2 Heat Transfer Coefficient

**Figs. 9-14** show relationship between heat transfer coefficient and heat flux at the location of downstream center for Experiments A to C.

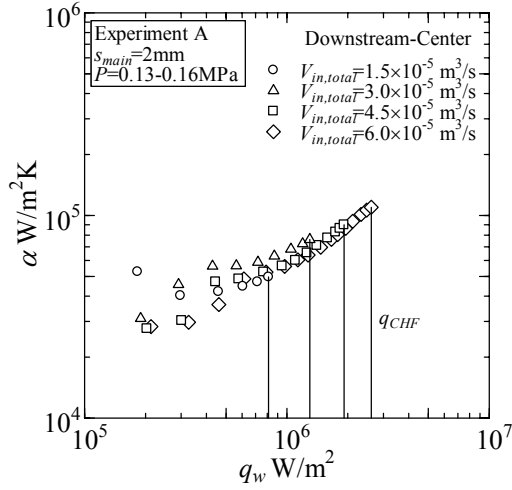


**Fig.9** Heat transfer coefficient for 2mm gap size in Experiment A.

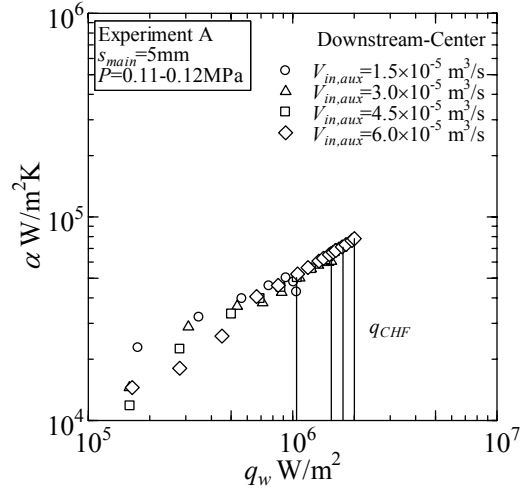


**Fig.12** Heat transfer coefficient for 5mm gap size in Experiment A.

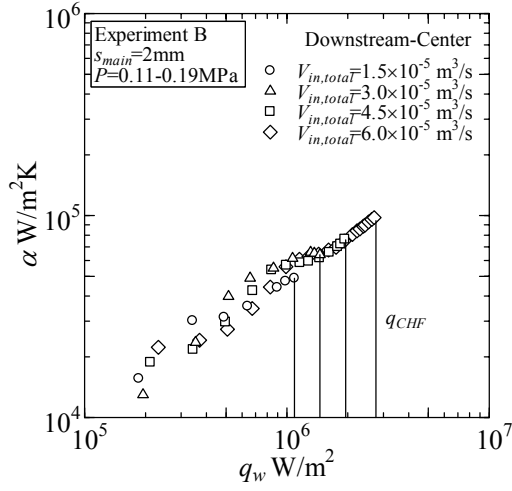


**Fig.10** Heat transfer coefficient for 2mm gap size in Experiment B.

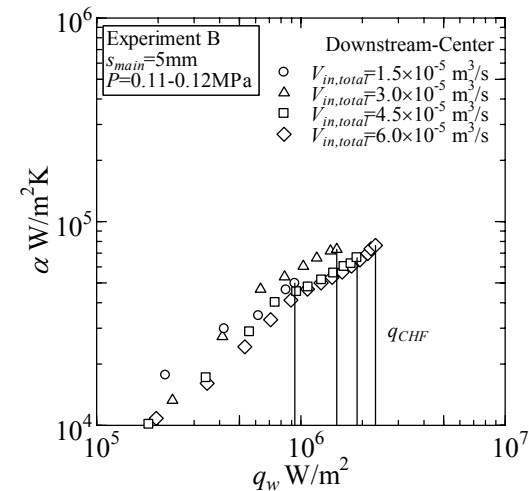


**Fig.13** Heat transfer coefficient for 5mm gap size in Experiment B.

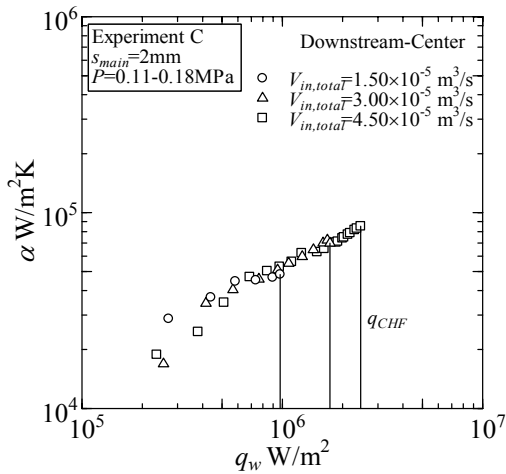


**Fig.11** Heat transfer coefficient for 2mm gap size in Experiment C.

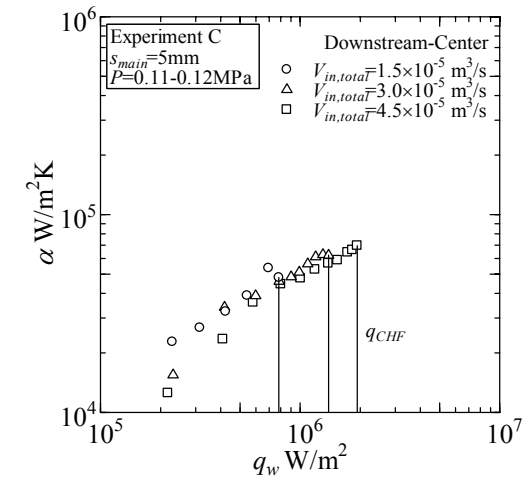


**Fig.14** Heat transfer coefficient for 5mm gap size in Experiment C.

For all experiments, heat transfer coefficients have an order of  $10^4$ - $10^5$  W/m<sup>2</sup>K. Highest values of heat transfer coefficient are obtained at heat flux just before CHF. The existence of grooves on the heating surface realizes the high values of heat transfer coefficient and prevents the deterioration of their values near CHF.

### 4.3 Performance Index

Liquid flow rate or mass velocity is one of key parameters to evaluate the performance of cold plates. Lower flow rate decreases the pump power and the liquid inventory, which contributes the reduction of energy consumption in the platforms and the reduction of launch mass and volume. A performance index  $\epsilon_{total}$  is defined here as

$$\epsilon_{total} = V_{in,total} / V_{min} \quad (1)$$

where,  $V_{min}$ : minimum volumetric flow rate to evaporate all liquid at the exit of the heated channel under critical heat flux m<sup>3</sup>/s, where vapor quality of unity is assumed at the exit. Therefore, the index shows a value of excessive liquid flow rate. Small values of  $\epsilon_{total}$  are required for the development of high performance cold plates. To take account of variation in the size of heating surface, inlet liquid velocity and subcooling,  $V_{min}$  in eq.(1) is represented by

$$V_{min} = q_{CHF} A_o / \{ \rho_l ( h_{fg} + c_{pl} \Delta T_{sub,in} ) \} \quad (2)$$

where,  $q_{CHF}$ : critical heat flux W/m<sup>2</sup>,  $A_o$ : area of cooling surface m<sup>2</sup>,  $\rho_l$ : liquid density kg/m<sup>3</sup>,  $h_{fg}$ : latent heat of vaporization J/kg,  $c_{pl}$ : isobaric specific heat, J/kgK,  $\Delta T_{sub,in}$ : subcooling of inlet liquid K.

**Fig. 15** shows performance indexes versus total inlet volumetric flow rates. (i) In Experiments A to C, performance index increase with increasing total inlet volumetric flow rate for almost all experimental conditions. (ii) In Experiment A, the gap size of 5mm improves the performance at low volumetric flow rates ( $V_{in,total} = 1.5, 3.0 \times 10^{-5}$  m<sup>3</sup>/s), while the gap size of 2mm provides better performance at high volumetric flow rates ( $V_{in,total} = 4.5, 6.0 \times 10^{-5}$  m<sup>3</sup>/s). (iii) The lowest performance index, i.e. highest performance in

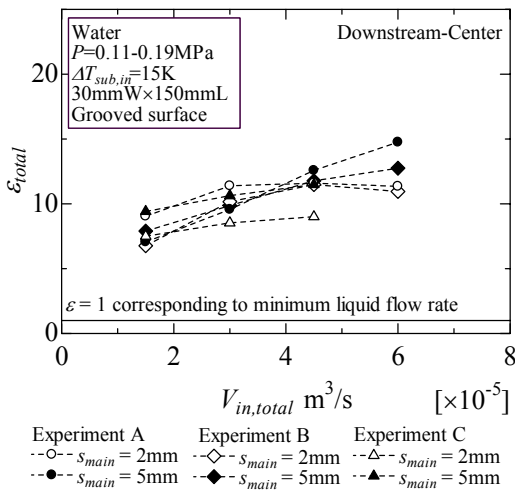


**Fig.15** Performance index versus total inlet volumetric flow rate of liquid.

Experiments A to C is obtained for the lowest volumetric flow rate  $V_{in,total} = 1.5 \times 10^{-5}$  m<sup>3</sup>/s tested here and gap size of 2mm in Experiment B. (iv) For  $V_{in,total} = 3.0, 4.5 \times 10^{-5}$  m<sup>3</sup>/s, the performance of gap size 2mm in Experiment C is clearly higher than others (performance index is smaller).

**Fig. 16** shows the relationship between performance index and critical heat flux. (v) In the case of  $q_{CHF}$  larger than  $1.7 \times 10^6$  W/m<sup>2</sup>, the gap size of 2mm in Experiment C gives higher performance than others. This tendency is related to the pressure distribution in the test section in Experiment C as mentioned later in section 4.4.

### 4.4 Protection of Burnout Occurring at Downstream in the Main Heated Channel

As mentioned in (v) in section 4.1, the method of liquid supply in Experiment C is superior to those in Experiments A and B from a viewpoint of increasing CHF value. The method prevents the occurrence of burnout in the downstream of the main heated channel. This is closely related to the transition of pressure distribution in both channels by increasing heat flux. As heat flux is increased, frictional pressure drop of two phase mixtures in the main heated channel is increased, while the gravitational pressure drop is decreased by the increase of void fraction. **Fig. 17** shows relationship between pressure drop in the main channel and heat flux for gap size of 2mm in Experiment C. As the heat flux is increased, frictional pressure drop becomes dominant in the total pressure drop. This phenomenon is evident for 2mm gap size conditions due to higher flow velocity of mixtures.

As mentioned above, pressure drop due to two-phase mixtures in the main heated channel is increased at higher heat flux, while the change in pressure drop in the auxiliary channel remains small. Therefore, the pressure difference between the auxiliary

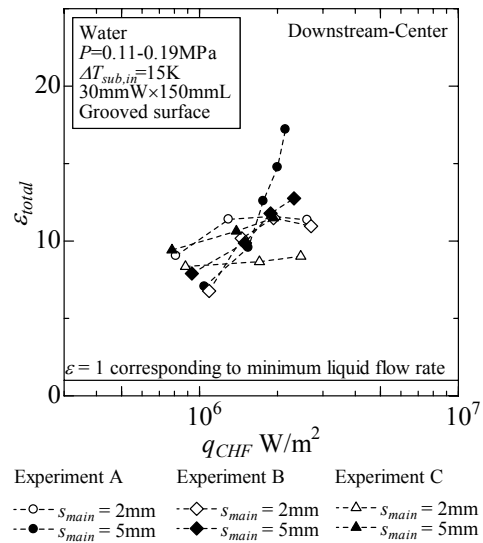


**Fig.16** Performance index versus critical heat flux.

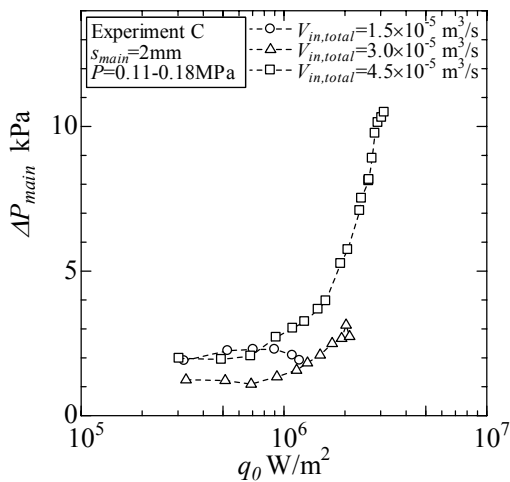


Fig.17 Pressure drop in main heated channel.

channel and the main heated channel is larger in downstream as expected in Fig.3 under high heat flux conditions. As a consequence, additional liquid supply is promoted in downstream to prevent burnout.

## 5. Conclusions

To develop cooling methods under extremely difficult conditions, i.e., at very high heat flux from a very large area, are required for the thermal management system in the laser-SSPS, flow boiling experiments to clarify the performance of a devised structure of cold plates with narrow channels were performed on ground by using water near atmospheric pressure. Three different methods of liquid supply to the devised structure composed of a main heated channel and an auxiliary unheated channel were tested. The following results

were obtained when liquid is supplied to both channels keeping the exit of auxiliary channel closed. (i) CHF values more than  $2 \times 10^6 \text{ W/m}^2$  were obtained at low total volumetric flow rate of  $4.5 \times 10^{-5} \text{ m}^3/\text{s}$  for 2mm gap size in the main heated channel. (ii) The performance of 2mm gap size is higher than that for 5mm gap size at  $V_{in,total} = 3.0, 4.5 \times 10^{-5} \text{ m}^3/\text{s}$ . (iii) CHF value tends to be higher than that obtained from previous studies because the additional liquid supply is promoted in downstream at higher heat fluxes corresponding to the pressure distributions in both channels.

## Acknowledgment

This research was supported by a Grant-in-Aid for Scientific Research (B) (No.18360103) from the Japan Society for the Promotion of Science. The authors express gratitude for the financial support.

## References

- 1) Monde, M., Kusuda, H. and Uehara, H., *J. Heat Transfer*, **104**, 300, 1982.
- 2) Bonjour, J. and Lallemand, M., *Int. Comm. Heat Mass Transfer*, Vol.24, No.2, pp.191, 1997.
- 3) Zhang, H., Mudawar, I. and Hasan, M.M., *Int. J. Heat and Mass Transfer*, **45**, 4079, 2002.
- 4) Kim, Y.H., Kim, S.J., Kim, J.J., Noh, S.W., Suh, K.Y., Rempe, J.L., Cheung, F.B. and Kim, S.B., *Int. J. Multipha. Flow*, **31**, 618, 2005.
- 5) Ohta, H., Shinmoto, Y., Ishikawa, Y. and K. Arika, *Proc.13th Int. Heat Transfer Conf.*, CD-ROM, BOI-32, 12, 2006.
- 6) Suzuki, K., Kawamura, H., Ishizuka, M., Iwasaki, H. and Kawano, K., *Proc. 6th ASME-JSME Joint Thermal Eng. Conf.*, TED-AJ03-106, CD-ROM, 2003.
- 7) Abe, Y., Tanaka, K., Yokoyama, T. and Iwasaki, A., *Proc. Int. Mech. Eng. Conf. Anaheim*, IMECE2004-61328, 2004.